RESEARCH ARTICLE

Essentiality of Succinate Dehydrogenase in *Mycobacterium smegmatis* and Its Role in the Generation of the Membrane Potential Under Hypoxia

Ildiko Pecsi,[a] Kiel Hards,[a] Nandula Ekanayaka,[a] Michael Berney,[a,b] Travis Hartman,[b] William R. Jacobs Jr.,[b] Gregory M. Cook[a,c]

University of Otago, Department of Microbiology and Immunology, Dunedin, New Zealand[a]; Department of Microbiology and Immunology, Albert Einstein College of Medicine, The Bronx, New York, USA[b]; Maurice Wilkins Centre for Molecular Biodiscovery, The University of Auckland, Auckland, New Zealand[c]

I.P. and K.H. contributed equally to this work.

ABSTRACT **Succinate:quinone oxidoreductase (Sdh) is a membrane-bound complex that couples the oxidation of succinate to fumarate in the cytoplasm to the reduction of quinone to quinol in the membrane. Mycobacterial species harbor genes for two putative *sdh* operons, but the individual roles of these two operons are unknown. In this communication, we show that *Mycobacterium smegmatis* mc²155 expresses two succinate dehydrogenases designated Sdh1 and Sdh2. Sdh1 is encoded by a five-gene operon (MSMEG_0416-MSMEG_0420), and Sdh2 is encoded by a four-gene operon (MSMEG_1672-MSMEG_1669). These two operons are differentially expressed in response to carbon limitation, hypoxia, and fumarate, as monitored by *sdh* promoter-*lacZ* fusions. While deletion of the *sdh1* operon did not yield any growth phenotypes on succinate or other nonfermentable carbon sources, the *sdh2* operon could be deleted only in a merodiploid background, demonstrating that Sdh2 is essential for growth. Sdh activity and succinate-dependent proton pumping were detected in cells grown aerobically, as well as under hypoxia. Fumarate reductase activity was absent under these conditions, indicating that neither Sdh1 nor Sdh2 could catalyze the reverse reaction. Sdh activity was inhibited by the Sdh inhibitor 3-nitroproprionate (3NP), and treatment with 3NP dissipated the membrane potential of wild-type or Δ*sdh1* mutant cells under hypoxia but not that of cells grown aerobically. These data imply that Sdh2 is the generator of the membrane potential under hypoxia, an essential role for the cell.**

IMPORTANCE **Complex II or succinate dehydrogenase (Sdh) is a major respiratory enzyme that couples the oxidation of succinate to fumarate in the cytoplasm to the reduction of quinone to quinol in the membrane. Mycobacterial species harbor genes for two putative *sdh* operons, *sdh1* and *sdh2*, but the individual roles of these two operons are unknown. In this communication, we show that *sdh1* and *sdh2* are differentially expressed in response to energy limitation, oxygen tension, and alternative electron acceptor availability, suggesting distinct functional cellular roles. Sdh2 was essential for growth and generation of the membrane potential in hypoxic cells. Given the essentiality of succinate dehydrogenase and oxidative phosphorylation in the growth cycle of *Mycobacterium tuberculosis*, the potential exists to develop new antituberculosis agents against the mycobacterial succinate dehydrogenase. This enzyme has been proposed as a potential target for the development of new chemotherapeutic agents against intracellular parasites and mitochondrion-associated disease.**

Received 20 June 2014 **Accepted** 16 July 2014 **Published** 12 August 2014

Citation Pecsi I, Hards K, Ekanayaka N, Berney M, Hartman T, Jacobs WR, Jr, Cook GM. 2014. Essentiality of succinate dehydrogenase in *Mycobacterium smegmatis* and its role in the generation of the membrane potential under hypoxia. mBio 5(4):e01093-14. doi:10.1128/mBio.01093-14.

Editor Eric Rubin, Harvard School of Public Health **Invited Editor** Kyu Rhee, Weill Cornell Medical College

Address correspondence to Gregory M. Cook, gregory.cook@otago.ac.nz.

The genus *Mycobacterium* comprises a group of obligately aerobic bacteria that have adapted to inhabit a wide range of intracellular and extracellular environments. A fundamental feature of this adaptation is the ability to respire and generate energy from variable sources or to sustain metabolism in the absence of growth. To achieve this, mycobacteria use a respiratory chain that consists of two types of NADH dehydrogenase (types I and II), multiple succinate dehydrogenases/fumarate reductases (FRDs), a menaquinol (MQH_2)-cytochrome *c* oxidoreductase termed the bc_1 complex, and two terminal respiratory oxidases, an aa_3-type cytochrome *c* oxidase (encoded by *ctaBCDE*) belonging to the heme-copper respiratory oxidase family and a cytochrome *bd*-type MQH_2 oxidase (*cydABCD*) (1–5). The regulator(s) and molecular signals that control the expression of these complexes in response to environmental change remain unknown.

Succinate dehydrogenase forms complex II of the respiratory chain and couples oxidative phosphorylation to central carbon metabolism by being an integral part of the citric acid cycle (6). Succinate dehydrogenase couples the oxidation of succinate to fumarate in the cytoplasm to the reduction of quinone to quinol in the membrane. The reverse reaction can be catalyzed by fumarate reductase, which is generally found in anaerobic or facultative anaerobes that utilize low-potential quinols (MQH_2 $E^{o\prime} = -74$ mV) to reduce fumarate as the final step in the anaerobic

electron transport chain (7–9). Succinate dehydrogenase and fumarate reductase have the same overall structural architecture (10, 11), and the reaction catalyzed (i.e., succinate oxidation or fumarate reduction) cannot be predicted solely on the basis of the primary amino acid sequence of the enzyme subunits. In general, increased reaction rates and catalytic efficiency in a particular direction reflect whether the enzyme is a succinate dehydrogenase or a fumarate reductase (12, 13).

Both succinate dehydrogenase and fumarate reductase consist of a large soluble domain and a smaller membrane-bound domain (membrane anchor) (10, 11). The soluble domain contains two hydrophilic subunits designated A and B. Flavoprotein subunit A contains a covalently bound flavin adenine dinucleotide (FAD) cofactor and the catalytic substrate-binding site. Subunit B is a small iron-sulfur protein containing three distinct iron-sulfur clusters that mediate electron transfer between the flavin and quinone catalytic sites in the membrane-bound domain. Subunits A and B have high sequence similarity between different bacterial species. The smaller membrane-bound domain varies between bacterial species consisting of one large or two small hydrophobic subunits designated C or C and D. Variation also occurs in the number of heme *b* groups (none, one, or two) and the type of quinone used (menaquinone or ubiquinone) (14).

Most mycobacterial genomes harbor two annotated succinate dehydrogenases, designated Sdh1 and Sdh2 (15). The oxidation of succinate to fumarate ($E^{o\prime} = +30$ mV) and reduction of ubiquinone to ubiquinol ($E^{o\prime} = +113$ mV) is a thermodynamically favorable reaction ($\Delta G^{\circ} = -15$ kJ/mol). In mycobacteria, the oxidation of succinate to fumarate ($E^{o\prime} = +30$ mV) is coupled to menaquinone reduction to MQH_2 ($E^{o\prime} = -74$ mV), an endergonic reaction under standard conditions ($\Delta G^{\circ} = +21$ kJ/mol) (16). How this thermodynamically unfavorable reaction is driven in mycobacteria is not known. In *M. smegmatis*, two putative operons for succinate dehydrogenase are present, Sdh1 (MSMEG_0416-MSMEG_0420) and Sdh2 (MSMEG_1672-MSMEG_1669) (15). These *M. smegmatis sdh* operons are contiguous with the two annotated *sdh* operons of *M. tuberculosis* designated Sdh1 (*Rv0249c-Rv0247c*) and Sdh2 (*Rv3316-Rv3319*). *M. smegmatis* does not harbor genes for fumarate reductase, making it a genetically tractable model to dissect the roles of the individual *sdh* operons. Here, we report that the *sdh1* and *sdh2* operons of *M. smegmatis* are differentially expressed in response to carbon limitation, hypoxia, and fumarate. Sdh1 was nonessential for growth, but Sdh2 was essential and generates the membrane potential under hypoxia.

RESULTS

***M. smegmatis* expresses two distinct succinate dehydrogenase operons** The operon structure of the two putative succinate dehydrogenases in *M. smegmatis* was determined by reverse transcriptase PCR (RT-PCR) with appropriate controls (Fig. 1A). On the basis of these data, we confirmed the operons as *sdh1* (MSMEG_0420-MSMEG_0416) (Fig. 1B, top panel) and *sdh2* (MSMEG_1672-MSMEG_1669) (Fig. 1B, bottom panel). BLAST searches based on the predicted translation products determined that the operon structure of *sdh2* is similar to that of the canonical *Escherichia coli* succinate:quinone oxidoreductase (SQR) enzyme in that it contains a putative catalytic flavoprotein subunit (Sdh2A), a soluble iron-sulfur cluster protein (Sdh2B), and two integral membrane subunits (Sdh2C and Sdh2D) (Fig. 1B). *sdh1*, on the other hand, is operonic with two unknown hypothetical proteins (MSMEG_0420 and MSMEG_0416) and has an integral membrane protein that appears to be a fusion of the expected two membrane subunits (Sdh1D) (Fig. 1B). These differences between the Sdh1 and Sdh2 operon structures suggest that they may play distinct cellular and energetic roles.

Sdh1 and Sdh2 protein sequence alignments show differences in heme-binding and catalytic residues. Using the functional classification of Hågerhåll (17), the *M. smegmatis* Sdh1 and Sdh2 enzymes are succinate:menaquinone oxidoreductases and belong to subclass 3. These enzymes are characterized by the oxidation of succinate coupled to the reduction of a low-potential quinone (menaquinone) in the respiratory chain. On the basis of their membrane-bound domain (subunit C or subunits C and D) and heme content, succinate dehydrogenases can be classified into five different types (18–20). According to this classification, Sdh2, with its two heme groups and two small hydrophobic subunits (subunits C and D) (Fig. 1B), can be classified as type A, previously reported in some extremophiles (21). Sdh1, with its large single hydrophobic subunit, C (Sdh1D) (Fig. 1B), can be classified as a type B enzyme; type B enzymes are found in a wide variety of microorganisms (reviewed in reference 14). Given that the operon structure of Sdh1 is similar to that of SQR subclasses known to have different numbers of hemes involved in quinone interactions (22), we made protein sequence alignments of Sdh1D and Sdh2D to representative SQR/MQH_2:fumarate oxidoreductase (QFR) sequences with experimentally determined numbers of hemes and also with the SQR- and QFR-encoding genes found in *M. tuberculosis* and other members of the family *Corynebacterineae* (see Fig. S1 and S2 in the supplemental material). We aligned only Sdh1D with other fused subunits and Sdh2D with other nonfused subunits to avoid erroneous alignments. It has been previously determined that conserved histidines are required for the binding of heme molecules proximal and distal to the cytoplasmic membrane interface (23) and so used this to make predictions of the heme contents of Sdh1 and Sdh2.

Sdh2D and Sdh1D appeared to have histidines that aligned in a pattern consistent with the presence of both a proximal and a distal heme (see Fig. S1 and S2). In addition, other closely related *Corynebacterineae* species (*Gordonia*, *Nocardia*, and *Rhodococcus*) displayed high sequence identity with Sdh1 homologues, including the conserved histidine positions. This prediction suggests that Sdh1 and Sdh2 may have structural specializations to facilitate interactions with menaquinones, relative to bacteria containing differing types of quinone. Alignments of Sdh2C and other C subunits gave the same result as Sdh2D alignments (data not shown). We aligned mycobacterial flavoprotein SdhA subunits with those of *E. coli*. It has been previously shown that differences in the FAD-binding site correspond to either efficient SQR or efficient QFR activity (13). Correspondingly, the known fumarate reductase in *M. tuberculosis* has the glutamate required for efficient *E. coli* QFR activity (see Fig. S3), as does the mycobacterial Sdh1. Sdh2 has a glutamine that is required for efficient SQR activity in *E. coli*. These analyses point to biochemical differences in *M. smegmatis* Sdh1 and Sdh2 that may relate to the physiological function of each enzyme and the conditions under which they operate.

***sdh-lacZ* transcriptional fusions are differentially regulated in response to energy limitation, hypoxia, and fumarate.** To facilitate the design of *sdh-lacZ* fusions, the transcriptional start sites

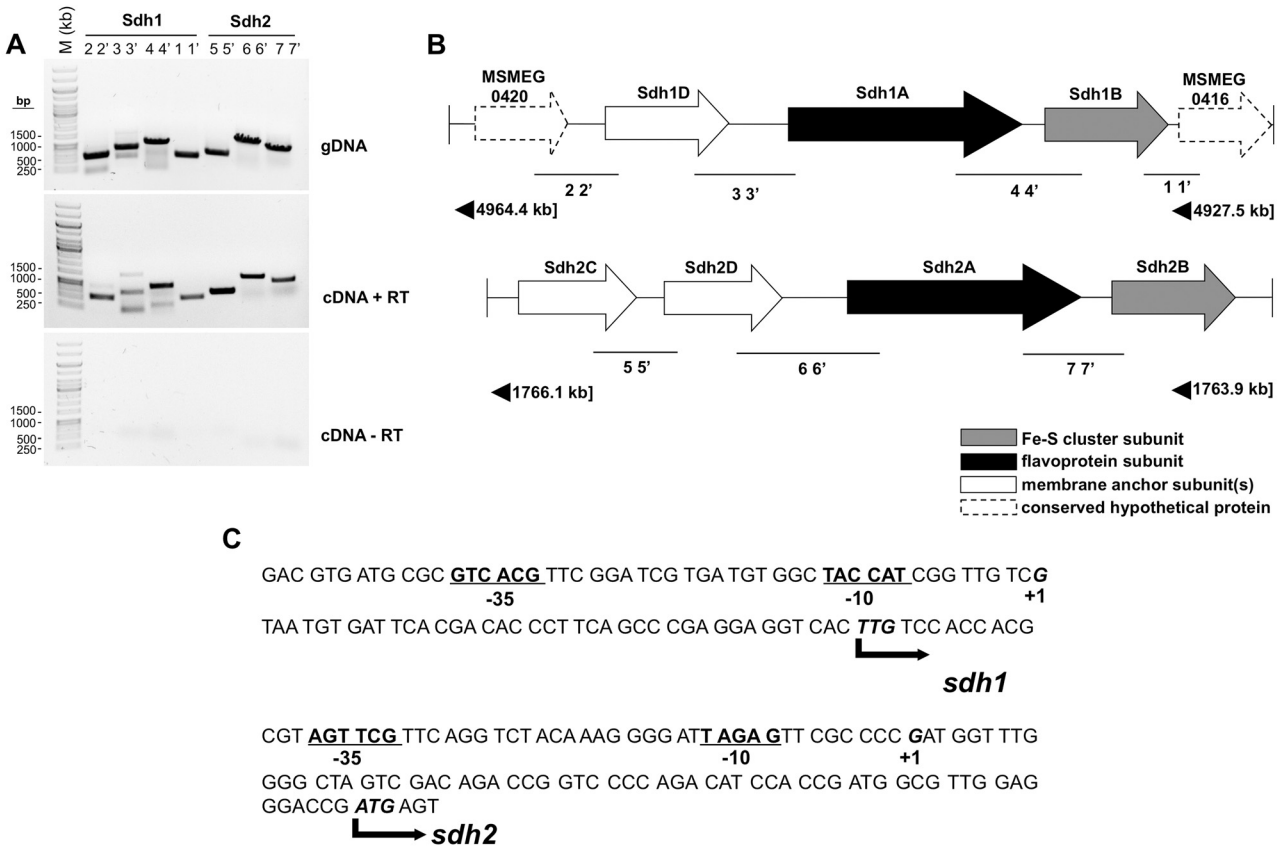

FIG 1 Transcriptional organization and start site mapping of *sdh1* and *sdh2* gene clusters in *M. smegmatis*. (A) Gels showing RT-PCR products encompassing the start, end, and intergenic region of two adjacent genes. Numbers above lanes correspond to amplified regions indicated in panel B. Each primer pair (see Table S2 in the supplemental material) was tested with the genomic DNA (gDNA) (top gel), cDNA synthesized with RT (cDNA + RT) (middle gel), and a control reaction mixture excluding RT (bottom gel) (cDNA-RT). Lane M, 1-kb DNA ladder molecular size marker. (B) Schematic view of the *sdh1* (MSMEG_0416-MSMEG_0420) and *sdh2* (MSMEG_1672-MSMEG_1669; *sdh2C-sdh2B*) gene clusters, including the predicted function of each subunit. (C) Upstream nucleotide sequence illustration showing the TSSs of *sdh1* and *sdh2*, located 39 and 62 bp upstream from the TTG and ATG codons (labeled +1 and in bold), respectively, identified by 5′ RACE. Bold and underlined −10 and −35, promoter elements.

(TSSs) of the *sdh1* and *sdh2* operons were determined by 5′ rapid amplification of cDNA ends (RACE) (Fig. 1C). Using this information, we constructed *sdh1*- and *sdh2-lacZ* transcriptional promoter fusions and studied operon promoter expression in response to carbon limitation (succinate) and oxygen limitation (hypoxia) (Fig. 2). When cells were grown aerobically (normoxia) with succinate (30 mM) as the sole carbon and energy source, *sdh1-lacZ* expression increased in response to the depletion of succinate (Fig. 2A). The expression of *sdh2-lacZ* remained relatively unchanged throughout the growth cycle (Fig. 2B). Under hypoxia (oxygen limitation), with succinate-replete conditions, the expression of *sdh1-lacZ* remained relatively constant during the growth cycle (Fig. 2C), while *sdh2-lacZ* expression increased in response to hypoxia (Fig. 2D).

Fumarate reductase and succinate dehydrogenase are closely related enzymes, and the preferred reaction catalyzed cannot be predicted on the basis of the amino acid sequence alone. The effect of fumarate on *sdh* expression was investigated under normoxic and hypoxic conditions (Fig. 3). When cells were grown on glycerol, *sdh1-lacZ* expression was repressed by the addition of fumarate under both normoxic and hypoxic conditions (Fig. 3A). In contrast, the expression of *sdh2-lacZ* was increased by the addition of fumarate under both normoxic and hypoxic conditions (Fig. 3B).

The *sdh2* operon is essential for *M. smegmatis* growth. To dissect the roles of Sdh1 and Sdh2, we attempted to create gene deletions of both *sdh* operons. For deletion of *sdh1*, a markerless deletion construct to replace the entire *sdh1* operon was made and introduced into *M. smegmatis* as described in the legend to Fig. 4. Single-crossover (SCO) and double-crossover (DCO) events were screened by PCR and Southern hybridization (Fig. 4C). The increased size of the left flank product in a DCO event indicated successful deletion of the *sdh1* operon, thereby showing that this operon is nonessential for the growth of *M. smegmatis*.

Using a similar strategy (Fig. 4B), Δ*sdh2* mutants could not be isolated. A total of 82 potential DCO events were screened, and 74 were found to be wild-type (WT) DCOs while the other 8 proved to be spontaneous sucrose-resistant SCO strains. Screening was also performed with medium supplementation with either succinate or fumarate (1 to 30 mM concentrations of each were tested); however, this could not rescue the lethal *sdh2* phenotype. The fact that we could not isolate an *sdh2* deletion mutant suggested that the *sdh2* operon might be essential for *M. smegmatis* growth. To confirm the essentiality of *sdh2*, we constructed a merodiploid

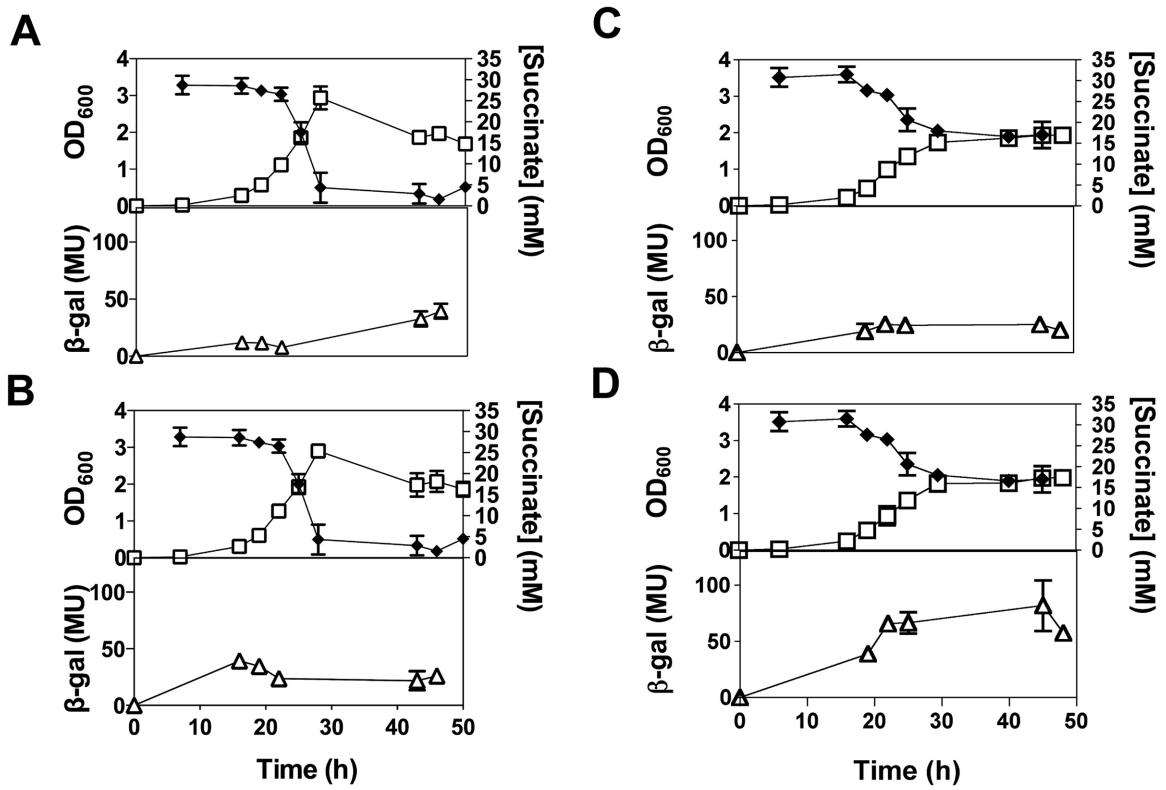

FIG 2 Levels of *sdh1-lacZ* and *sdh2-lacZ* expression in *M. smegmatis*. *M. smegmatis* cells were grown in HdB minimal medium supplemented with 30 mM succinate under normoxic (conical flasks) or hypoxic (stoppered serum vials) conditions. Hypoxic conditions were achieved at approximately 25 to 30 h, as indicated by methylene blue decolorization. The graphs show how *sdh1-lacZ* expression under normoxic (A) and hypoxic (C) conditions and *sdh2-lacZ* expression under normoxic (B) and hypoxic (D) conditions affect OD_{600} (open squares), the succinate concentration (solid diamonds), and β-galactosidase (β-gal) activity (in Miller units [MU]; open triangles). The experiments were carried out in biological triplicate, and the results shown are mean values and standard deviations. The empty vector pJEM15 was used as a control and gave no detectable activity (data not shown).

strain carrying an additional copy of the *sdh2* operon expressed from its native promoter by using the mycobacteriophage L5-based integrating pUHA267 vector, which integrates into the *attB* chromosomal site of the genome. We integrated this complementing vector into the SCO strain and screened for DCO events in this merodiploid background. Of 26 potential DCOs screened at the native locus, 25 were of the WT and one *sdh2* deletion mutant was isolated, which was confirmed by the smaller size of a left flank product than that of the WT in a Southern blot assay (Fig. 4D). This shows that the *sdh2* operon can be deleted at its native locus but only if a functional copy of the *sdh2* operon is supplied elsewhere on the chromosome; therefore, we conclude that the *sdh2* operon is essential for the growth of *M. smegmatis*.

We analyzed the Δ*sdh1* mutant for a growth phenotype over a

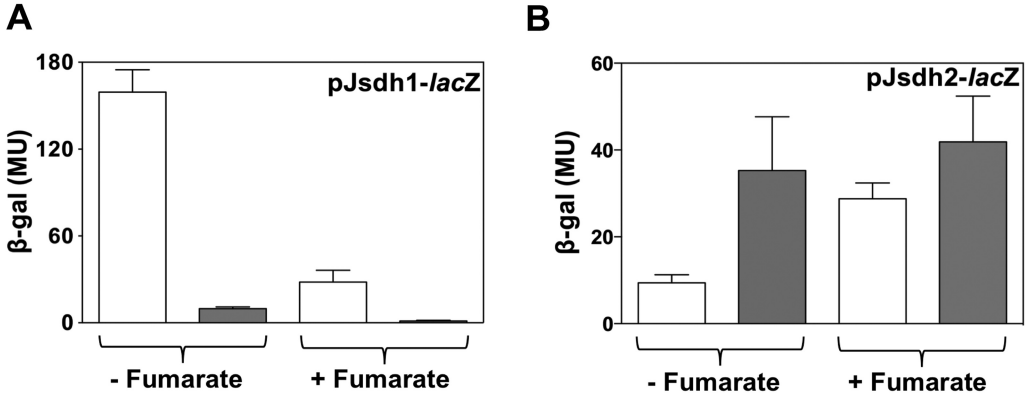

FIG 3 Effect of fumarate on *sdh1-lacZ* and *sdh2-lacZ* expression. *M. smegmatis* cells were grown in HdB minimal medium supplemented with 0.2% glycerol with (+) or without (−) 30 mM fumarate under normoxic (open bars) or hypoxic (gray bars) conditions. Panels: A, *sdh1-lacZ* expression; B, *sdh2-lacZ* expression. The experiments were carried out in biological triplicate, and the results shown are mean values and standard deviations. MU, Miller units; β-gal, β-galactosidase.

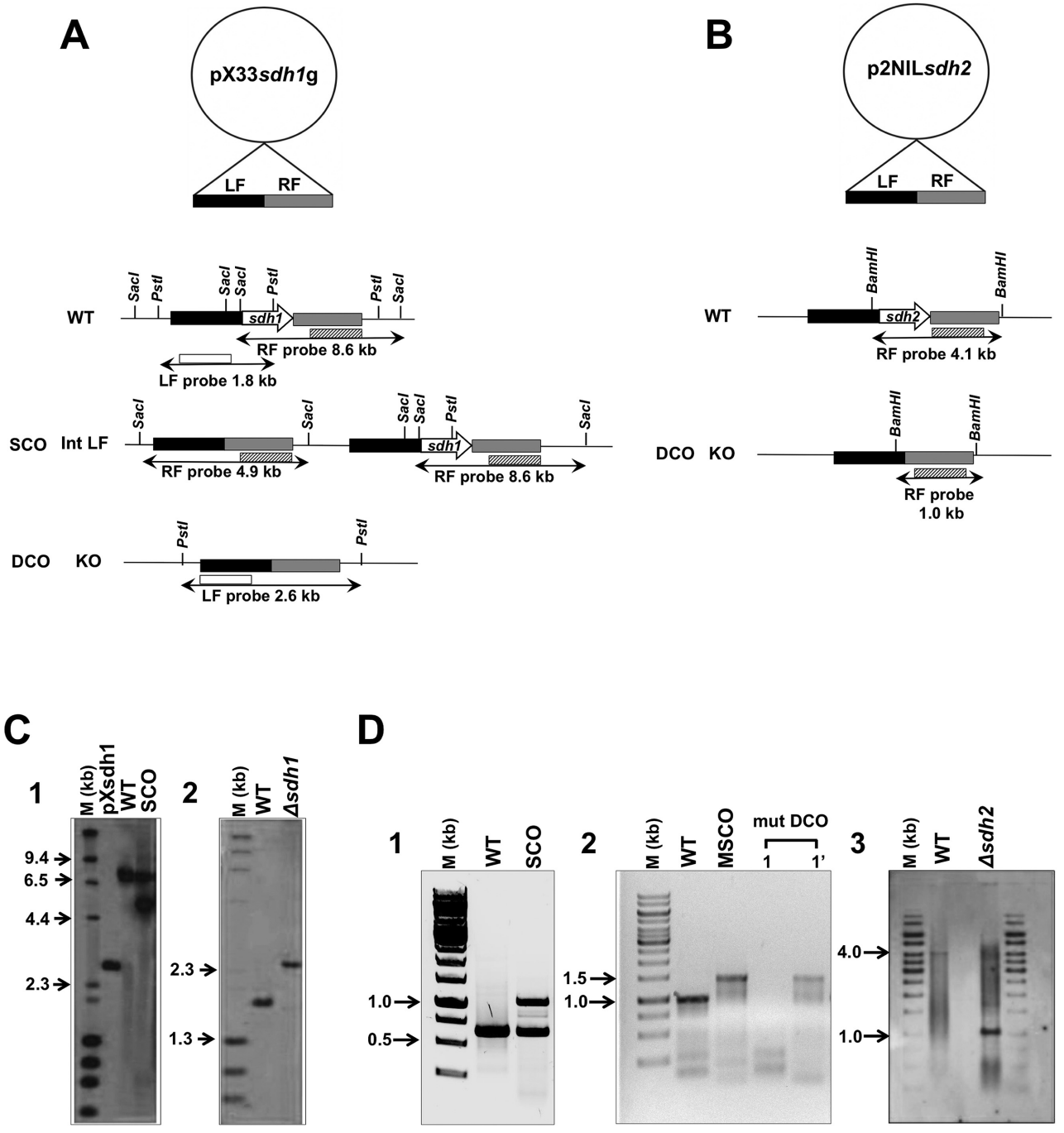

FIG 4 Construction of markerless *sdh1* and *sdh2* operon deletion mutants of *M. smegmatis*. Schematic diagrams of the vectors pX33*sdh1*g (A) and p2NIL*sdh2* (B) with the left flank (LF) and right flank (RF) of the *sdh1* and *sdh2* operons, integration of the suicide vector into the chromosome, and subsequent deletion of the *sdh1* and *sdh2* operons are shown. Relevant restriction sites: SacI for SCO event and PstI for DCO event screens for the *sdh1* operon; BamHI for the DCO event screen for the *sdh2* operon. Fragment sizes detected by Southern hybridization are indicated. KO, knockout. Southern blot analysis of pX33*sdh1*g vector integration due to a SCO event (C1) yielding the 4.9-kb fragment (lane SCO). The WT *M. smegmatis* chromosomal DNA, yielding an 8.6-kb fragment, was used as a positive control (lane WT). Plasmid pXsdh1 was also used as a control (lane pXsdh1). Confirmation of *sdh1* operon nonessentiality (C2). The probe used to perform the hybridization contained the 1.8-kb WT and 2.6-kb deletion mutant *sdh1* operon (Δ*sdh1*) restriction fragments, respectively. Lanes M, HindIII-digested λ DNA molecular size marker (D1). Identification of *sdh2* SCO strain by colony PCR. SCO strains were generated by homologous recombination of p2Nbk-*sdh2* with a chromosomal copy of the *sdh2* operon. Chromosomal DNA of *M. smegmatis*, yielding the 0.6-kb fragment (lane WT), was used as a positive control; the p2NIL*sdh2* vector integration due to a SCO event yielded the 1.0-kb fragment (lane SCO) (D2). Colony PCR of the generated DCO strain. Lanes 1 and 1′ represent samples from the same cell line. The potential DCO cell lines were screened for both the WT copy (designated 1) and the *sdh2* operon deletion mutant (designated 1′). The lengths of the expected PCR products for the WT and deletion mutant *sdh2* operons were 0.9 and 1.4 kb, respectively. A merodiploid SCO (MSCO) strain was used as a positive control (D3). A Southern blot analysis of the mutant (mut) DCO strain is shown. The probe used to perform the hybridization contained the 4.1-kb WT and 1.0-kb deletion mutant *sdh2* operon (Δ*sdh2*) restriction fragments, respectively. Lanes M, 1-kb DNA ladder molecular size marker. Drawings are not to scale.

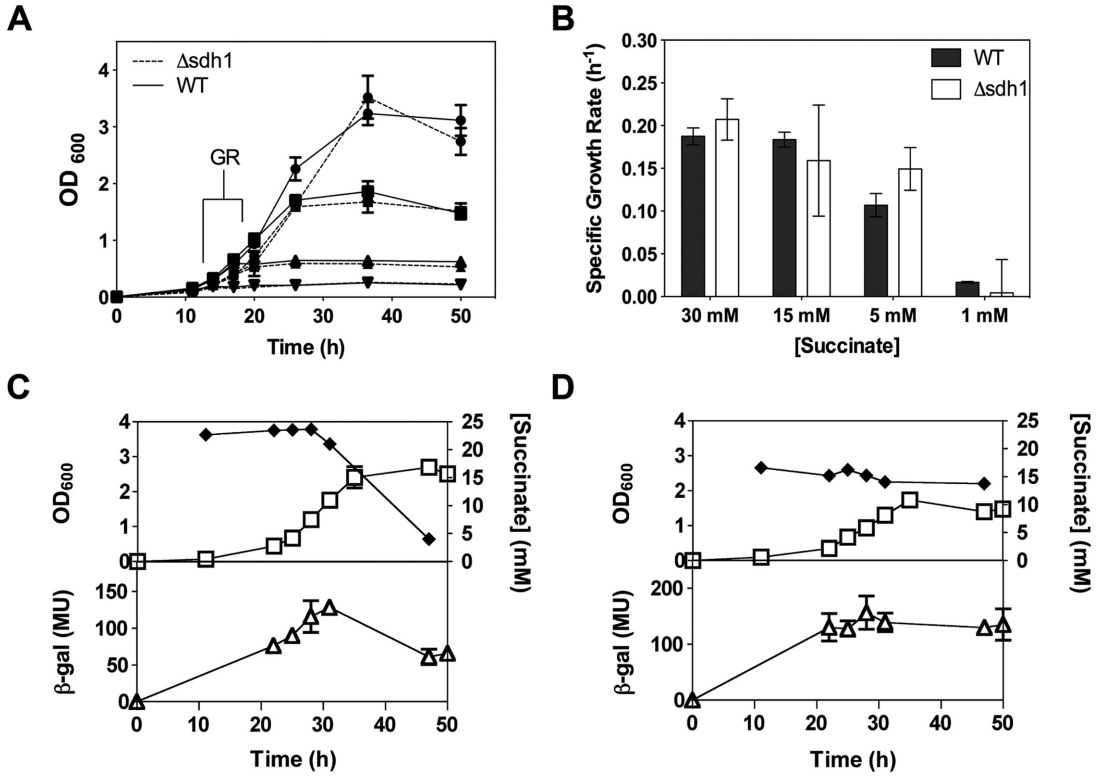

FIG 5 Growth and *sdh2-lacZ* expression of Δ*sdh1* mutant. Shown are the growth curves (A) and plotted growth rates (B) of the WT (solid lines and filled bars) and the Δ*sdh1* deletion mutant (dotted lines and open bars) in HdB minimal medium under normoxic conditions with succinate at 30 mM (closed circles), 15 mM (closed squares), 5 mM (closed triangles), and 1 mM (inverted closed triangles). The specific growth rate was calculated between the two time points indicated in panel A. (C and D) Expression levels of *sdh2-lacZ* in the *M. smegmatis* Δ*sdh1* mutant grown under normoxic (C) or hypoxic (D) conditions in HdB minimal medium supplemented with 30 mM succinate. (D) Hypoxic conditions were achieved at approximately 30 h, as indicated by methylene blue decolorization. OD_{600} (open squares), succinate concentration (solid diamonds), β-galactosidase (β-gal) activity (in Miller units [MU]; open triangles) are shown. The experiments were carried out in biological triplicate, and the results shown are mean values and standard deviations.

wide range of succinate concentrations (Fig. 5A and B). No significant differences in growth rate or yield (final optical density at 600 nm [OD_{600}]) were observed. We rationalized that this was due to upregulation (compensation) of Sdh2 in the Δ*sdh1* background. To test this hypothesis, we measured the expression of *sdh2-lacZ* in a Δ*sdh1* mutant background (Fig. 5C and D) and compared it to *sdh2-lacZ* expression in WT cells (Fig. 2B and D). The expression of *sdh2-lacZ* was elevated in the Δ*sdh1* mutant background relative to that in the WT background under both normoxic and hypoxic growth conditions (compared Fig. 5C and D with 2B and D), suggesting that Sdh2 was compensating for the loss of Sdh1 in *M. smegmatis* during growth on succinate.

Enzyme activities of the Sdh1 and Sdh2 complexes in *M. smegmatis*. In order to understand the biochemical differences between WT *M. smegmatis* and the Δ*sdh1* mutant; we prepared inverted (inside-out) membrane vesicles (IMVs) of both WT and Δ*sdh1* mutant cells grown under both normoxic and hypoxic conditions on succinate (Hartman's de Bont [HdB] minimal medium). We assayed for Sdh activity by using the dye-based phenazine ethosulfate (PES)–2,6-dichlorophenolindophenol (DCIP) assay (24) with appropriate *E. coli* controls (positive and negative) to validate our enzyme assays (Fig. 6A and B). IMVs of *E. coli* exhibited high rates of succinate dehydrogenase activity and succinate-dependent oxygen consumption (Fig. 6A and B). Both enzyme activities were essentially absent from an *E. coli* Δ*frdABCD* Δ*sdhABCD* double mutant (strain RP437; see Table S1 in the supplemental material) and well above WT levels in *E. coli* strains overexpressing either the SQR operon (pFAS, $SdhABCD^+$) or the QFR operon (pH3, $FrdABCD^+$) (Fig. 6A and B). IMVs prepared from *M. smegmatis* cells grown aerobically had similar kinetics of succinate oxidation, regardless of the presence or absence of Sdh1 (Fig. 6C). IMVs prepared from Δ*sdh1* mutant cells grown under hypoxic conditions exhibited a 2-fold lower apparent V_{max} than WT cells (Fig. 6D; see Table S3). The apparent K_m values for succinate were consistently lower in the Δ*sdh1* mutant than in the isogenic WT parent, suggesting a higher affinity for succinate oxidation in the Δ*sdh1* genetic background (see Table S3).

To determine if the *M. smegmatis* Sdh enzymes are capable of fumarate reduction, we assayed for fumarate reductase activity in mycobacterial IMVs. A direct assay for fumarate reductase activity in mycobacteria has not been previously reported in the literature. We used a benzyl viologen (BV) assay that has been described for use with the *E. coli* QFR enzyme (13). We validated that the assay was correctly working by detecting fumarate reductase activity in *E. coli* IMVs that were either WT or overexpressing the *E. coli* QFR (DW35 pH3 $FrdABCD^+$) (Fig. 7). Consistently, an *E. coli* Δ*frdABCD* Δ*sdhABCD* double mutant (strain RP437) gave no detectable activity. Furthermore, we were able to detect fumarate reductase activity in IMVs prepared from *M. bovis* BCG (Fig. 7). However, we were unable to detect any fumarate reductase activ-

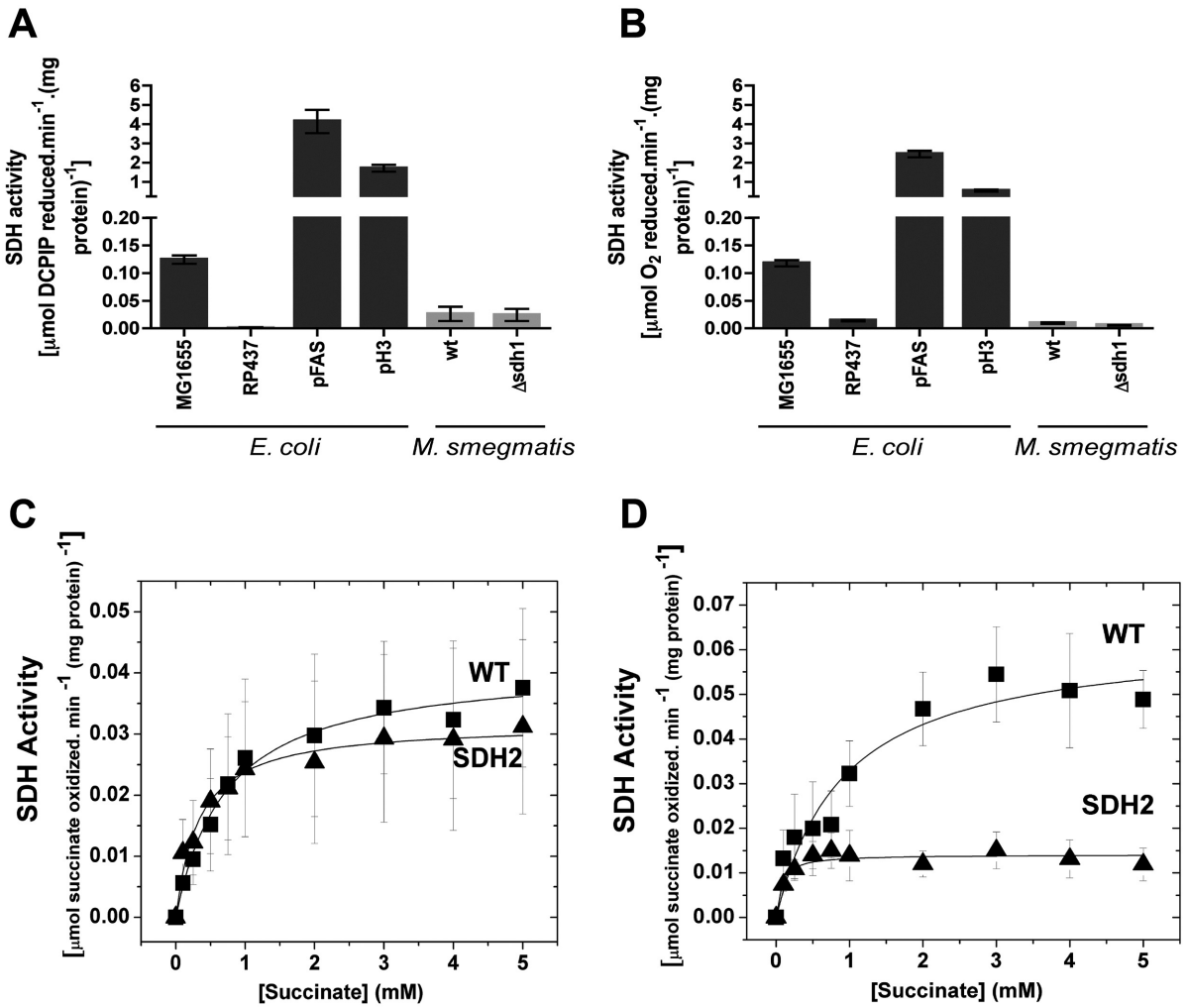

FIG 6 Kinetic characterization of succinate oxidation by IMVs of WT and Δ*sdh1* mutant *E. coli* and *M. smegmatis*. Succinate dehydrogenase activities in IMVs of WT and Δ*sdh1* mutant *E. coli* and *M. smegmatis* strains were measured with the PES-DCIP assay (A) or a Clark O_2 electrode-based method (B). IMVs of *E. coli* were prepared from cells grown aerobically in LB medium at 37°C. MG1655, *E. coli* WT; RP437, *E. coli* Δ*frdABCD* Δ*sdhABCD* double mutant; pFAS, *E. coli* overexpressing the *sdhABCD* operon; pH3, *E. coli* overexpressing the *frdABCD* operon. (C and D) Rates of succinate oxidation by WT and Δ*sdh1* mutant *M. smegmatis* IMVs prepared from cells grown under normoxic (C) and hypoxic (D) conditions in HdB minimal medium supplemented with 30 mM succinate. Data were analyzed by nonlinear least-squares regression of the Michaelis-Menten equation with GraphPad Prism 6, and V_{max} and K_m data are summarized in Table S3 in the supplemental material. WT, solid squares; SDH2 (Δ*sdh1* deletion mutant strain), solid triangles. Error bars indicate the standard error of a biological triplicate.

ity in IMVs prepared from WT or Δ*sdh1* mutant *M. smegmatis* grown under any of the conditions used in this study (Fig. 7).

Sdh2 is the generator of the membrane potential under hypoxia. To understand the importance of succinate oxidation in *M. smegmatis*, we determined the contributions of succinate oxidation to the membrane potential ($\Delta\psi$) and proton gradient (ΔpH). Succinate oxidation coupled to proton translocation was measured by using acridine orange (AO) quenching in IMVs prepared from *M. smegmatis* cells grown under normoxia or hypoxia on succinate (Fig. 8). In these experiments, succinate was provided as the electron donor for the electron transport chain. Succinate oxidation to fumarate results in the generation of MQH_2, which is then used by either the proton-pumping MQH_2-cytochrome *c* oxidoreductase bc_1-aa_3-type cytochrome *c* oxidase (bc_1-aa_3 pathway) and/or non-proton-translocating cytochrome *bd*-type MQH_2 oxidase (1, 2). Succinate oxidation by either WT or Δ*sdh1* mutant IMVs resulted in significant proton pumping (AO quenching), which was reversed by the protonophore *m*-chlorophenylhydrazone (CCCP), demonstrating that succinate oxidation was coupled to proton pumping by the bc_1-aa_3 pathway (Fig. 8). Lower levels of succinate-driven proton pumping (quenching) were observed in WT cells grown under hypoxia (Fig. 8, trace c) than in the Δ*sdh1* mutant grown under the same conditions (Fig. 8, trace d).

Succinate dehydrogenase activity in *M. tuberculosis* is inhibited by 3-nitroproprionate (3NP) (25), which is a complex II-specific suicide inhibitor (26). We validated this as an inhibitor of Sdh activity in *M. smegmatis* (see Fig. S4 in the supplemental material) and used it to study the effect of 3NP treatment on the generation of the electrical potential across the cell membrane ($\Delta\Psi$) in whole cells. When WT or Δ*sdh1* mutant cells were grown under normoxia in the presence of 3NP (400 μM), the growth rate and final

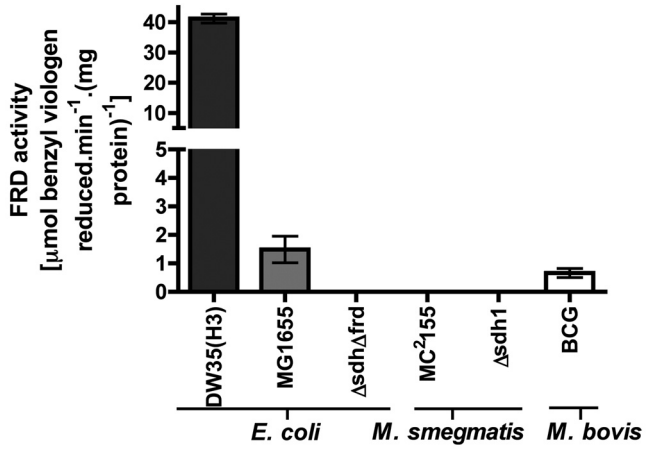

FIG 7 Fumarate reductase activities in *E. coli*, *M. bovis* BCG, and *M. smegmatis* IMVs. Fumarate reductase (FRD) activities (in μmol of BV oxidized min^{-1} mg of $protein^{-1}$) were calculated with BV as the electron donor (0.2 mM) under anaerobic conditions. No fumarate reductase activity could be detected in IMVs prepared from *M. smegmatis* cells grown under either normoxic or hypoxic conditions on HdB minimal medium supplemented with 30 mM succinate. IMVs of *E. coli* and *M. bovis* BCG were prepared from cells grown aerobically in LB and 7H9 media with ADS at 37°C. DW35(H3), *E. coli* overexpressing the *frdABCD* operon; MG1655, *E. coli* WT; *E. coli* Δ*frdABCD* Δ*sdhABCD* double mutant (RP437). Fumarate (5 mM) was present in each assay. Error bars indicate the standard error of a technical triplicate.

OD_{600} were the same as those of untreated cells (Fig. 9A and B). The same strains grown under hypoxia in the presence of 3NP showed some growth inhibition, and the final OD_{600} was always lower in the 3NP-treated cells, particularly for the Δ*sdh1* mutant (Fig. 9C and D). To determine the effect of 3NP on succinate dehydrogenase inhibition and electron transport chain activity, we measured the $\Delta\psi$ under these conditions. Under normoxic growth conditions, the $\Delta\psi$ was comparable between WT and Δ*sdh1* mutant cells (170 mV) and 3NP treatment had no significant effect on the $\Delta\psi$ (Fig. 9E, cells sampled at 48 h) (*P* value, >0.05; 95% confidence interval [CI], one-way analysis of variance [ANOVA]), suggesting that generation of the membrane potential under these conditions was not dependent on succinate or was a minor contributor. Under hypoxic conditions, the $\Delta\psi$ was significantly dissipated by 3NP (*P* value, <0.001 for WT untreated versus 3NP-treated cells; *P* value, <0.01 for Δ*sdh1* untreated versus 3NP-treated cells, 95% CI, one-way ANOVA) in both the WT and Δ*sdh1* mutant. Taken together, these data suggest that succinate oxidation (Sdh activity) was responsible for generation of the $\Delta\psi$ under hypoxia but not under normoxia and was not dependent on the presence of the *sdh1* operon for this activity.

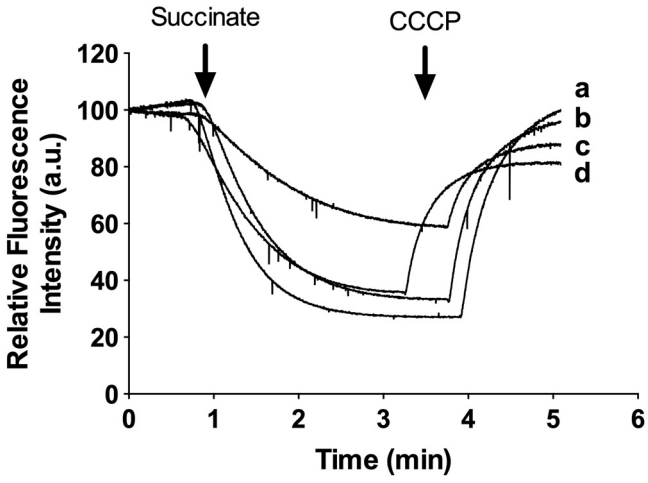

FIG 8 Succinate-driven proton translocation in IMVs of *M. smegmatis* (WT versus Δ*sdh1* mutant). Quenching of AO fluorescence in IMVs was initiated with 5 mM succinate, and at the indicated time points, the uncoupler CCCP at 50 μM was added to collapse the proton gradient (reversal of AO fluorescence). IMVs were prepared from *M. smegmatis* cells grown under normoxic (traces a and b) or hypoxic (traces c and d) conditions in HdB minimal medium supplemented with 30 mM succinate. Traces were normalized to a starting value of 100 arbitrary units (a.u.). Experiments are representative of a technical triplicate. Traces: a, WT cells grown under normoxic conditions; b, Δ*sdh1* mutant cells grown under normoxic conditions; c, WT cells grown under hypoxic conditions; d, Δ*sdh1* mutant cells grown under hypoxic conditions.

DISCUSSION

Members of the genus *Mycobacterium* harbor two copies of the succinate dehydrogenase operon designated *sdh1* and *sdh2*, but the reasons for this remain unclear. In this communication, we report that the *sdh* operons of *M. smegmatis* are differentially expressed in response to energy and oxygen limitations and fumarate, suggesting distinct cellular and energetic roles. The *sdh1* operon was upregulated in response to energy limitation (normoxic conditions, high proton motive force) and downregulated in response to hypoxia and fumarate (Fig. 10). Sdh1 was dispensable for growth, and no phenotype for the Δ*sdh1* mutant was identified. In contrast, Sdh2 was downregulated in response to energy limitation and upregulated in response to hypoxia (low proton motive force) and fumarate (Fig. 10). The *sdh* expression data obtained with *sdh-lacZ* fusions were consistent with microarray data obtained for the *sdh1* and *sdh2* genes, when bacteria were grown in continuous culture in response to the growth rate and hypoxia (15). Exogenous fumarate addition induced *sdh2* expression, even though Sdh2 was without measured fumarate reductase activity. One possible reason for this increased *sdh2* expression is that fumarate accumulation signals hypoxia to *M. smegmatis*. The fact that fumarate addition increased *sdh2* expression under both normoxic and hypoxic conditions supports this hypothesis.

Sdh2 was essential for growth, even in an $Sdh1^+$ background, demonstrating that Sdh1 was unable to compensate for Sdh2 activity in *M. smegmatis*. The essentiality of Sdh enzymes for mycobacterial growth has previously been reported in a transposon site hybridization (TraSH) screening of *M. tuberculosis* that showed that Sdh1, but not Sdh2, is essential for optimal growth under aerobic conditions on standard laboratory medium (27). In contrast, TraSH screening selecting for *M. tuberculosis* mutants that continue to replicate under hypoxic conditions found that *sdh2* mutants were overrepresented, suggesting that Sdh2 has a pivotal role in the transition of *M. tuberculosis* from aerobic to hypoxic conditions (28). The reasons for this essentiality, despite the presence of one intact copy of an *sdh* operon, has not been investigated.

The *M. smegmatis* Sdh1 and Sdh2 enzymes are succinate: menaquinone oxidoreductases. The oxidation of succinate to fumarate ($E^{o\prime} = +30$ mV) coupled to menaquinone reduction to MQH_2 ($E^{o\prime} = -74$ mV) is an endergonic reaction under standard conditions ($\Delta G^{\circ} = +21$ kJ/mol) (16), and therefore, these bacte-

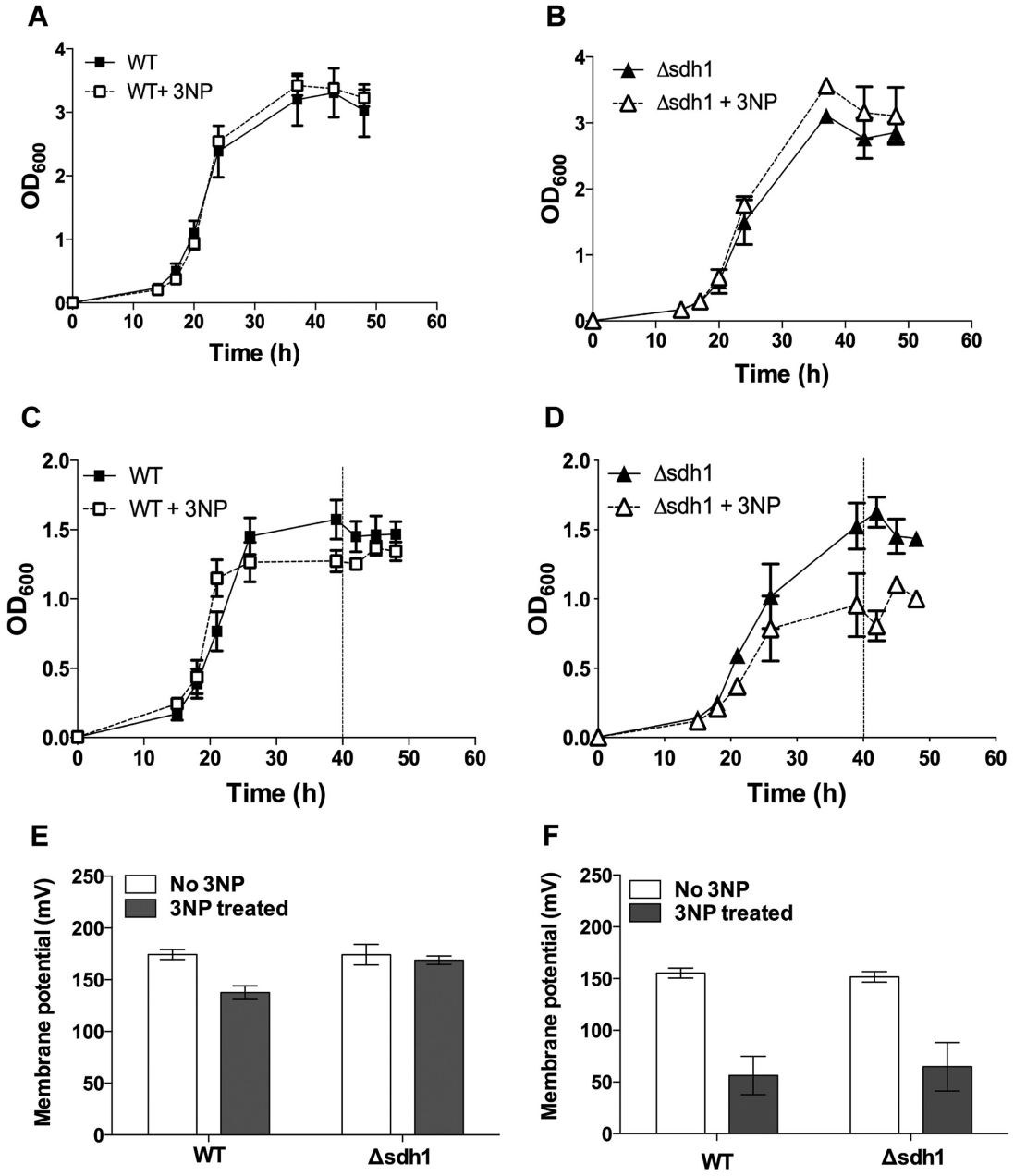

FIG 9 Effect of 3NP on the growth and membrane potential of the WT and the Δ*sdh1* mutant. Cells (WT, squares; Δ*sdh1* mutant, triangles) were grown under normoxic (A and B) or hypoxic (C and D) conditions in HdB minimal medium with 30 mM succinate in the absence or presence of 400 μM 3NP. The dotted vertical line (approximately 40 h) indicates the point at which methylene blue was decolorized and hence hypoxic conditions were achieved. At 48 h of growth, the membrane potential from normoxic (E) and hypoxic (F) cells was determined as described in Materials and Methods. Error bars represent the standard deviation (A to D) or the standard error (E and F) of a biological triplicate. Ethanol was used as the vehicle in all of the experiments.

ria face a thermodynamic problem. *Bacillus* species also use succinate:menaquinone oxidoreductases, and in *Bacillus subtilis* and *Bacillus licheniformis*, the endergonic succinate dehydrogenase reaction is driven by the proton motive force (29–31). The succinate-menaquinone reductases generally contain two heme *b* groups in the membrane anchor (14) (Fig. 10). These hemes are referred to as the proximal heme (b_P), located close to the negative side of the membrane (near the hydrophilic subunits), and the distal heme (b_D), close to the positive side of the membrane near the menaquinone-binding site. The hemes differ in redox potential, with heme b_P having a high potential (e.g., $E^{o\prime} = +42$ mV in *B. subtilis*) and heme b_D having a low potential (e.g., $E^{o\prime} = -131$ mV in *B. subtilis*) (19, 22, 30, 32). Mutations in the axial ligands (His-28 and His-113) for heme b_D in *B. subtilis* lead to impaired electron transfer from succinate to menaquinone, demonstrating that heme b_D is essential for electron transfer to menaquinone (32). In mycobacterial Sdh, a similar pair of histidines are found at His-65 to His-113 (Sdh1, *M. smegmatis* numbering) and His-65 to His-107 (Sdh2, *M. smegmatis* numbering) for potential heme *b* ligation, suggesting that this adaptation is

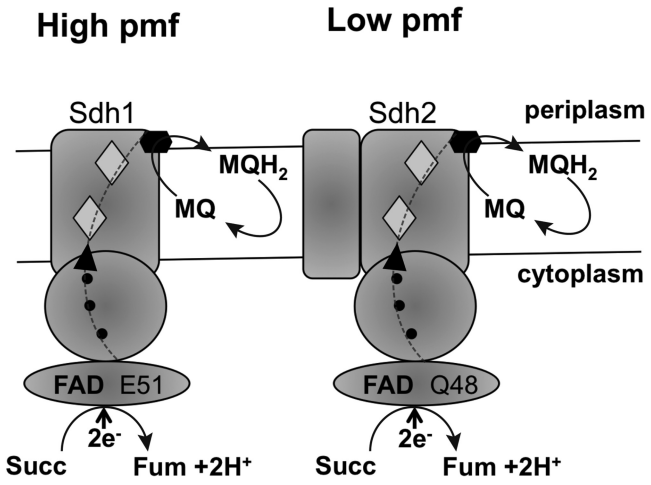

FIG 10 Schematic diagram outlining the subunit structures and proposed functions of Sdh1 and Sdh2 in *M. smegmatis*. Sdh1 is expressed under normoxia (high proton motive force [pmf]), and Sdh2 is expressed under hypoxia (low pmf). Both enzymes catalyze the oxidation of succinate (Succ) to fumarate (Fum) and the two-electron ($2e^-$, dotted line) reduction of menaquinone (MQ) to MQH_2. Sdh1 is composed of three subunits (A, B, and D, type A enzyme), and Sdh2 is a four-subunit enzyme (A to D, type B enzyme). Shaded diamonds represent proposed proximal and distal hemes in the membrane anchor domain. Solid circles indicate proposed iron-sulfur clusters in subunit B. The solid hexagon is a proposed menaquinone-binding site.

conserved in the mycobacterial Sdh enzymes. Neither the Sdh1 nor the Sdh2 enzyme was able to catalyze the reduction of fumarate to succinate under the conditions tested. Our data support a model in which Sdh1 is adapted to high redox potentials (normoxic conditions) and Sdh2 is adapted to low redox potentials (hypoxic conditions) (Fig. 10). Such adaptations have been linked to the FAD cofactor of SQR/QFR in *E. coli*. The redox potentials of the FAD in SQR and QFR are −138 and −122 mV, respectively (13). Analysis of the amino acids of SQR and QFR involved in flavin binding has shown that in *E. coli* FrdA, Glu-49 is located close to the FAD cofactor and in *E. coli* SdhA, a Gln-50 residue is found at this position (13). Replacement of these residues with the residue found in the complementary enzyme (i.e., FrdA E49Q or SdhA Q50E) results in the enzyme becoming more efficient in the opposite direction (13). In mycobacterial Sdh1, Sdh2, and fumarate reductase enzymes, these same residues are conserved: SdhA1 Glu-51, SdhA2 Gln-48, and *M. tuberculosis* Frd Glu-51 (see Fig. S3 in the supplemental material). These observations raise the possibility that the reduction potential of the FAD is different in *M. smegmatis* Sdh1 and Sdh2, consistent with the enzymes functioning under different redox potentials. On the basis of *E. coli* data, one might speculate that *M. smegmatis* Sdh1 is more akin to QFR than Sdh2, which resembles SQR of *E. coli*.

The reason for the essentiality of Sdh2 in *M. smegmatis* remains unknown. Our data demonstrate an essential role for Sdh2 in generating the membrane potential of *M. smegmatis* under hypoxia but not under normoxic conditions, suggesting that succinate is the preferred respiratory electron donor at low oxygen tensions in *M. smegmatis*. The succinate dehydrogenase inhibitor 3NP was without effect on *M. smegmatis* cells growing aerobically but caused some growth inhibition under hypoxia, suggesting that blocking succinate dehydrogenase has different implications for cells growing under normoxia or hypoxia. These data suggest different carbon flux through succinate under the two conditions and the essentiality of succinate dehydrogenase in membrane potential generation under hypoxia. We propose an energetic scheme for *M. smegmatis* in which Sdh2-mediated succinate oxidation generates a reduced MQH_2 pool that saturates the proton-pumping bc_1-aa_3 supercomplex, leading to the generation of the membrane potential and sustaining ATP synthesis under hypoxia. A similar mechanism has been proposed in *M. tuberculosis*, but the Sdh responsible for this process is not known (25). Rhee and coworkers (25) have proposed that succinate accumulation in *M. tuberculosis* during hypoxia plays an essential role in fueling Sdh activity to sustain the membrane potential, ATP synthesis, and anaplerosis. If oxygen is completely lacking, excess succinate may be secreted to sustain the membrane potential or stored to enable immediate resumption of growth when electron acceptors become available, akin to a metabolic battery (25). In our experiments, the membrane potential was still generated in hypoxic *M. smegmatis* cells even when the external succinate concentration was high (15 mM), indicating that the primary mechanism of membrane potential generation involved succinate oxidation coupled to proton pumping by the *bcc-aa*$_3$ complex and not succinate secretion *per se*. Our findings and those of others (25) are consistent with mitochondrial studies where respiratory succinate dehydrogenase (complex II) is the primary generator of the membrane potential and ATP levels under hypoxic conditions and is more efficient than complex I under these conditions (33). The use of succinate and Sdh2 by *M. smegmatis* to generate the membrane potential may explain why the proton-pumping NADH oxidoreductase complex I (*nuo* operon, NDH-1) is downregulated under hypoxic conditions in *M. smegmatis* (15). The use of Sdh2 in favor of NDH-1 under these conditions may well prevent the excess production of reactive oxygen species (ROS) mediated by complex I, a major contributor to ROS production in bacteria and mitochondria.

M. smegmatis lacks genes for a canonical fumarate reductase, and we could not detect fumarate reductase activity in cells grown under either normoxic or hypoxic conditions. We could readily detect fumarate reductase activity in *M. bovis* BCG cells. It has been proposed that fumarate may be an important endogenous electron acceptor for energy production and maintenance of redox balance (oxidation of NADH to NAD^+) in hypoxic nonreplicating mycobacteria (34) or used as a mechanism to generate succinate as an excreted end product for maintenance of the membrane potential (35). Interestingly, the use of fumarate as an electron acceptor in *E. coli* requires complex I, and expression of the *nuo* operon is stimulated by the presence of fumarate (7). This stands in direct contrast to *M. smegmatis*, where the *nuo* operon seems to be silent under hypoxic conditions (15).

Complex II plays an important role in the cellular physiology of eukaryotes and prokaryotes, and its malfunction has been associated with human disease (36, 37). The enzyme has been proposed as a potential target for the development of new chemotherapeutic agents against intracellular parasites (38) and mitochondrion-associated disease (39). Given the essentiality of succinate dehydrogenase and the importance of fumarate reductase in mycobacterial pathogens, the potential exists to develop new antituberculosis agents against these two respiratory complexes.

MATERIALS AND METHODS

Bacterial strains, media, and growth conditions. All of the strains and plasmids used in this study are listed in Table S1 in the supplemental material. Plasmid propagation was carried out with *E. coli* strains grown in Luria-Bertani (LB) medium at 37°C with agitation (200 rpm) or on LB 1.5% agar plates. *M. smegmatis* strain mc^{2}155 (40) and derived strains were routinely grown at 37°C with agitation (200 rpm) in HdB minimal medium (41) supplemented with 0.05% Tween 80 (Sigma-Aldrich). Where specified, 25 mM glycerol, 30 mM succinate, or 30 mM fumarate was used as the sole carbon and energy source. For allelic-exchange mutagenesis experiments, *M. smegmatis* mc^{2}155 was grown in Lemco medium with or without the addition of 15 g/liter Bacto agar as described previously (42). Kanamycin was added at 20 μg/ml for *M. smegmatis* and at 50 μg/ml for *E. coli*, and hygromycin B was added at 50 μg/ml for *M. smegmatis* and at 200 μg/ml for *E. coli*. Gentamicin was added at 5 μg/ml for *M. smegmatis* and at 20 μg/ml for *E. coli*. For sucrose selection, 10% (wt/vol) sucrose was included. X-Gal (5-bromo-4-chloro-3-indolyl-β-D-galactopyranoside) was used at 40 μg/ml. OD_{600}s of culture samples diluted in saline (0.85% NaCl) were measured in cuvettes with a 1-cm path length in a Jenway 6300 spectrophotometer.

Small-scale batch growth of *M. smegmatis* was carried out aerobically (normoxic) in either 125- or 250-ml conical flasks or under hypoxic conditions in 120-ml sealed serum vials (butyl rubber stoppered, O_2 impermeable). Oxygen depletion under hypoxia was confirmed by decolorization of methylene blue added (1.5 μM final concentration) (in a separate replicate) as previously described (43). Large-scale batch growth in either HdB containing 30 mM succinate (*M. smegmatis*) or LB (*E. coli*) for IMV preparations were carried out either aerobically in 2-liter conical flasks or under hypoxia in 2-liter Schott bottles (butyl rubber stoppered, O_2 impermeable). A 600-ml volume of medium was used in the Schott bottles, which is the same headspace/medium volume ratio as in serum vials. *M. bovis* BCG was maintained according to established protocols used for *M. tuberculosis* (44). Large-scale growth was carried out in 2-liter conical flasks of 7H9 medium supplemented with only the albumin and dextrose components (ADS) of oleic acid-albumin-dextrose-catalase.

RNA extraction and RT-PCR. Total RNA was extracted with TRIZOL reagent according to the manufacturer's instructions. Cell lysis was achieved by three cycles of bead beating in a Mini-Beadbeater (Biospec) at 5,000 rpm for 30 s. DNA was removed from the RNA preparation by treatment with 2 U of RNase-free DNase with the TURBO DNA-free kit (Ambion) according to the manufacturer's instructions. The quality of the RNA was checked on a 1.2% agarose gel, and the concentration was determined with a NanoDrop ND-1000 spectrophotometer. RT-PCR was performed with the SuperScript III RT kit (Invitrogen) according to the manufacturer's instructions for the RT step and the Phusion High-Fidelity PCR kit for the PCR step. The RT reactions were carried out with 1 μg of RNA template and gene-specific primers (listed in Table S2 in the supplemental material) that bind within the *sdh1* or *sdh2* operon, followed by PCR with the same set of primers, and 5 μl of the resulting RT reaction mixture were used.

DNA manipulation and cloning of constructs. All molecular biology techniques were carried out according to standard procedures (45). Amino acid sequences for the succinate dehydrogenases/fumarate reductases included in the analysis were obtained from the NCBI protein database and aligned with the Clustal Omega (46) server hosted at EMBL-EBI. Restriction or DNA-modifying enzymes and other molecular biology reagents were obtained from Roche Diagnostics or New England BioLabs. Genomic DNA of *M. smegmatis* was isolated as described previously (47). To create a markerless deletion of the *sdh1* operon, which corresponds to the MSMEG_0420-to-MSMEG_0416 gene region, a 1,017-bp fragment flanking MSMEG_ 0420 upstream and a 916-bp fragment flanking MSMEG_0416 downstream were amplified. The two products were fused by overlap extension PCR (48), cloned into the SpeI site of pPR23-derived (49) vector pX33 (47), creating pX*sdh1*g, and transformed into *M. smegmatis* mc^{2}155. The same procedure was used to create a markerless deletion of the *sdh2* operon, which corresponds to the MSMEG_1672-to-MSMEG_1669 gene region; a 1,230-bp fragment flanking MSMEG_1669 upstream and a 1,031-bp fragment flanking MSMEG_1672 downstream were amplified. The two products were fused by overlap extension PCR and cloned into the HindIII site of the p2NIL vector (50), creating p2NIL*sdh2*k, and transformed into *M. smegmatis* mc^{2}155. To make the complementing construct for *M. smegmatis* WT *sdh2*, the complete operon, together with the native promoter 352 bp upstream of *sdh2*, was PCR amplified. Thereafter, the 3.7-kb PCR product was cloned into the HindIII site of the integrative *E. coli-Mycobacterium* shuttle vector pUHA267 (51), creating plasmid pUHA267*sdh2*h (for the primers used, see Table S2 in the supplemental material). All constructs were verified by restriction digestion and sequencing.

Generation of *M. smegmatis sdh1* and *sdh2* deletion mutant strains. Allelic replacement of the *sdh1* operon was carried out essentially as previously described (49). In brief, a culture of *M. smegmatis* mc^{2}155 carrying pX*sdh1*g was grown at 28°C to an OD_{600} of approximately 0.6 to 0.8 and then plated onto LB medium with 0.05% Tween 80 (LBT) solid medium containing gentamicin, which selected for integration of the plasmid via a SCO event. Thereafter, colonies that formed a yellow product when exposed to 250 mM catechol were screened by Southern hybridization analysis for correct integration of the construct. One integrant was chosen and grown in 5 ml of LBT medium containing gentamicin, at 37°C. Aliquots of this culture were then plated onto low-salt LBT plates containing sucrose and incubated at 40°C to select for a DCO event resulting in loss of the plasmid and deletion of the *sdh1* operon. Colonies that did not form the yellow product after exposure to catechol were screened by Southern hybridization analysis for correct deletion of the *sdh1* operon.

For deletion of the *sdh2* operon, a two-step deletion strategy similar to that described by Parish et al. (50, 52) was used. A 5-μg UV-pretreated (53) p2NIL*sdh2*k plasmid sample was electroporated into competent *M. smegmatis*, and then SCO transformants were selected on medium containing kanamycin and X-Gal. Merodiploid strains were constructed by electroporation of the SCO strain with the complementing plasmid pUHA267*sdh2*h, followed by isolation of kanamycin- and hygromycin-resistant transformants. DCOs were generated in the WT and merodiploid backgrounds by streaking cells onto plates lacking antibiotics. DCO selection was performed on medium containing sucrose and X-Gal. Candidate clones (Hyg^r, Kan^s, and white color) were first screened by colony PCR with gene-specific screening primers (see Table S2 in the supplemental material) and then confirmed by Southern blotting to determine whether the WT or deletion mutant allele was present at the targeted chromosomal location. Southern blot hybridization analysis was carried out with the Amersham Gene Images AlkPhos Direct Labeling and detection system by using CDP-Star detection reagent (GE Healthcare) according to the manufacturer's instructions. Restriction digestion of the genomic DNA was performed with PstI, resulting in 1.8- and 2.6-kb fragments in the cases of WT and *sdh1* deletion strains, respectively, and with BamHI, resulting in 1.0- and 4.1-kb fragments in the cases of the WT and *sdh2* deletion strains, respectively. The probe used for *sdh1* was the 1.0-kb left flank fragment, and for *sdh2*, a 0.8-kb fragment was separately PCR amplified (for the primers used, see Table S2).

Mapping of *sdh1* and *sdh2* TSSs and construction of *sdh1-lacZ* and *sdh2-lacZ* transcriptional fusions. The TSSs of the *sdh1* and *sdh2* operons were mapped by 5′ RACE by using the components of a 3′/5′ RACE kit according to the manufacturer's instructions and as previously described (54), with the primers listed in Table S2 in the supplemental material.

To study *sdh1* and *sdh2* expression, transcriptional fusions of *sdh1* and *sdh2* operon promoters were cloned into pJEM15 (55), a plasmid containing a promoterless *lacZ* gene. PCR products of 607 and 654 bp encompassing the *sdh1* (−424 to +183) and *sdh2* (−453 to +201) promoter regions relative to the TSSs were amplified, respectively, with the primers listed in Table S2. Thereafter, the products were cloned into the BamHI and SphI sites of pJEM15, creating plasmids pJsdh1 and pJsdh2 (see Table S1). All of the promoter regions amplified by PCR were confirmed by

DNA sequencing. The plasmids were transformed into *M. smegmatis* mc^{2}155 by electroporation. The transcriptional activities of the *sdh1* and *sdh2* operons were determined with the β-galactosidase assay as described previously (47).

Preparation of IMVs. Cell suspensions from large-scale batch growth (~2-liter total volume) were pooled and centrifuged at 7,000 rpm for 15 min. The pellet was resuspended in lysis buffer (50 ml of 50 mM morpholinepropanesulfonic acid [MOPS; pH 7.5] buffer with 1 mM phenylmethylsulfonyl fluoride, 1 mM dithiothreitol [DTT], 1 Roche protease inhibitor tablet, 5 mM $MgCl_2$, 0.05% Tween 80, 2.5 mg/ml lysozyme, 2.5 mg DNase I). The cell suspension was homogenized four times with a homogenizer and incubated for 30 min on ice. The cells were broken by six passages through a precooled French pressure cell at 20,000 lb/in^2 (AMINCO). The lysate was centrifuged at 10,000 rpm at 4°C for 10 min to remove unbroken cells. The pellet was discarded. This step was repeated with this clarified lysate to ensure that no unbroken cells were carried over. The clarified lysate was centrifuged at 150,000 × *g* for 45 min at 4°C to harvest IMVs. The resulting membrane pellet was resuspended in lysis buffer that did not contain lysozyme or DNase I. Aliquots were used immediately or snap-frozen after 10% glycerol addition and stored at −80°C. Protein concentration was determined by using the bicinchoninic acid (BCA) reaction (Sigma) with bovine serum albumin as the standard.

Determination of succinate concentrations and succinate dehydrogenase and fumarate reductase assays. Cell suspensions sampled during growth were centrifuged at 13,000 × *g* for 1 min, and supernatant samples were stored at −20°C until used for analysis. Succinate concentrations were estimated with the Megazyme Succinate Acid Assay kit according to the manufacturer's instructions. Succinate dehydrogenase enzymes as isolated are partially deactivated by tightly bound oxaloacetate at their active sites, and thus, it is necessary to activate the enzyme to fully express their succino-oxidase activity (56, 57). To activate the enzyme, the membrane vesicles were incubated at 37°C for 5 min in 50 mM MOPS (pH 7.5) with 2 mM KCN and the desired amount of succinate. Activated membranes were then added, and the reaction was initiated by the addition of 660 μM PES and 50 μM DCIP. The reduction of DCIP was followed by measuring the absorbance at 600 nm of DCIP (ε^{600} = 19.1 mM^{-1} cm^{-1}) with a Varian Cary 50 spectrophotometer. Additional supplementation with fumarate or 3NP was performed as described in Results.

Fumarate reduction activities of IMVs were determined by measuring the fumarate-dependent oxidation of BV. This method has been previously described for assays of *E. coli* QFR and SQR (13). The assay mixture contained 50 mM Tris-HCl (pH 7.5), 1 mM DTT, 5 mM fumarate (pH 7.5), 0.2 mM BV, 60 μg/ml glucose oxidase, 4 μg/ml catalase, and 20 mM glucose. The Tris-HCl was boiled and then cooled under nitrogen, with the addition of DTT, to remove oxygen from the buffer before the addition of the other assay components. Glucose oxidase, catalase, and glucose were added to maintain anaerobiosis. Assay mixtures were prepared in 1.5-ml screw-top cuvettes under a flow of nitrogen. The desired amount of membrane vesicles was added, and then the assay was immediately initiated by the addition of a stoichiometric amount of sodium dithionite. The progress of the reaction was monitored by the decrease in BV absorbance at 602 nm (ε^{602} = 9.6 mM^{-1} cm^{-1}) (13). Rates were corrected for baseline activity, which was estimated in technical triplicate for each organism and membrane concentration used. Fumarate reductase activity was calculated as μmol of BV oxidized min^{-1} mg of $protein^{-1}$.

Measurement of oxygen consumption rates. A model 10 Clark-type oxygen electrode (Rank Brothers Ltd., Cambridge, England) linked to a PicoLog ADC-20 data logger was used to measure O_2 consumption in IMVs. IMVs were diluted to 0.5 mg/ml in 50 mM MOPS (pH 7.5) and supplemented with 5 mM succinate, with stirring, to initiate O_2 consumption. The electrode was calibrated daily by flushing 0.1 M K-phosphate buffer with gaseous N_2 for 5 min (oxygen solubility of 220 nmol/ml). Rates were normalized to the protein concentration of cell pellets estimated by using the BCA reaction (Sigma), which were lysed with 1 M NaOH with heating at 95°C and subsequently neutralized with 1 M HCl.

Membrane potential determination and proton-pumping assays. Determination of ΔΨ was performed as previously described (58). Cells (1 ml, grown under normoxic or hypoxic conditions, Fig. 9) were transferred to glass tubes (in triplicate) containing [^{3}H]methyltriphenylphosphonium iodide (TPP^+) (30 to 60 Ci $mmol^{-1}$) ([^{3}H]TPP^+, 2.4 nM final concentration). After incubation for 10 min at 37°C, the cultures were centrifuged through 0.35 ml of silicone oil (BDH Laboratory Supplies, Poole, England) in 1.5-ml microcentrifuge tubes (13,000 × *g*, 5 min, 22°C) and 20-μl samples of supernatant were removed. The tubes and contents were frozen (−20°C), and cell pellets were removed with dog nail clippers. The supernatant and cell pellets were dissolved in 2 ml of scintillation fluid (Amersham), and the amount of [^{3}H]TPP^+ taken up by the cells was determined with a Tri-Carb liquid scintillation analyzer (PerkinElmer). The silicone oil mixture was a 40% mixture of phthalic acid bis(2-ethyl-hexyl ester) and 60% silicone oil (40% part mixture of DC200/200 silicone oil and 60% DC 550). Silicone oils were left overnight at room temperature to equilibrate. The intracellular volume (3.45 ± 0.59 μl mg of $protein^{-1}$) was estimated from the difference between the partitioning of ^3H_2O and [^{14}C]taurine. The ΔΨ was calculated from the uptake of [^{3}H]TPP^+ according to the Nernst relationship. Nonspecific TPP^+ binding was estimated from cells that had been treated with valinomycin and nigericin (10 μM each) for 25 min (58).

Proton translocation into IMVs was determined by measuring the quenching of the fluorescent probe AO with a Cary Eclipse Fluorescence spectrophotometer. IMVs (0.5 mg/ml) were preincubated at 30°C in a weak buffer system consisting of 10 mM HEPES (pH 7.5), 100 mM KOH, and 5 mM $MgCl_2$ containing 5 μM AO for 2 min with constant stirring. The reaction was then initiated by adding 5 mM succinate as an electron donor. Once the fluorescence quenching reached a steady state, the proton gradient was collapsed by the addition of the uncoupler CCCP (50 μM). The excitation and emission wavelengths were 493 and 530 nm, respectively.

SUPPLEMENTAL MATERIAL

Supplemental material for this article may be found at http://mbio.asm.org/lookup/suppl/doi:10.1128/mBio.01093-14/-/DCSupplemental.

Figure S1, DOCX file, 0.2 MB.
Figure S2, DOCX file, 0.1 MB.
Figure S3, DOCX file, 0.1 MB.
Figure S4, DOCX file, 0.6 MB.
Table S1, DOCX file, 0.1 MB.
Table S2, DOCX file, 0.1 MB.
Table S3, DOCX file, 0.1 MB.
Text S1, DOCX file, 0.1 MB.

ACKNOWLEDGMENTS

I.P. was funded by a Health Sciences Career Development Postdoctoral Fellowships, University of Otago. K.H. is supported by the Otago Medical Research Foundation. M.B. was financially supported by a Marsden Grant from the Royal Society of New Zealand. G.M.C. was supported by a James Cook Fellowship from the Royal Society of New Zealand and the Health Research Council of New Zealand. W.R.J., an HHMI investigator, is funded by NIH/NIAID AI26170 and R01AI097548-01A1.

We thank Gary Cecchini and Elena Maklashina for supplying *E. coli* bacterial strains and their helpful comments regarding Sdh and Frd assays.

REFERENCES

1. **Cook GM, Berney M, Gebhard S, Heinemann M, Cox RA, Danilchanka O, Niederweis M.** 2009. Physiology of mycobacteria. Adv. Microb. Physiol. **55**:81–182, 318–189. http://dx.doi.org/10.1016/S0065-2911(09)05502-7.
2. **Boshoff HI, Barry CE, III.** 2005. Tuberculosis—metabolism and respiration in the absence of growth. Nat. Rev. Microbiol. **3**:70–80. http://dx.doi.org/10.1038/nrmicro1065.

3. **Weinstein EA, Yano T, Li LS, Avarbock D, Avarbock A, Helm D, McColm AA, Duncan K, Lonsdale JT, Rubin H.** 2005. Inhibitors of type II NADH:menaquinone oxidoreductase represent a class of antitubercular drugs. Proc. Natl. Acad. Sci. U. S. A. **102:**4548–4553. http://dx.doi.org/10.1073/pnas.0500469102.
4. **Kana BD, Weinstein EA, Avarbock D, Dawes SS, Rubin H, Mizrahi V.** 2001. Characterization of the *cydAB*-encoded cytochrome *bd* oxidase from *Mycobacterium smegmatis*. J. Bacteriol. **183:**7076–7086. http://dx.doi.org/10.1128/JB.183.24.7076-7086.2001.
5. **Matsoso LG, Kana BD, Crellin PK, Lea-Smith DJ, Pelosi A, Powell D, Dawes SS, Rubin H, Coppel RL, Mizrahi V.** 2005. Function of the cytochrome bc_1-aa_3 branch of the respiratory network in mycobacteria and network adaptation occurring in response to its disruption. J. Bacteriol. **187:**6300–6308. http://dx.doi.org/10.1128/JB.187.18.6300-6308.2005.
6. **Cecchini G.** 2013. Respiratory complex II: role in cellular physiology and disease. Biochim. Biophys. Acta **1827:**541–542. http://dx.doi.org/10.1016/j.bbabio.2013.02.010.
7. **Unden G, Bongaerts J.** 1997. Alternative respiratory pathways of *Escherichia coli*: energetics and transcriptional regulation in response to electron acceptors. Biochim. Biophys. Acta **1320:**217–234. http://dx.doi.org/10.1016/S0005-2728(97)00034-0.
8. **Unden G, Schirawski J.** 1997. The oxygen-responsive transcriptional regulator FNR of *Escherichia coli*: the search for signals and reactions. Mol. Microbiol. **25:**205–210. http://dx.doi.org/10.1046/j.1365-2958.1997.4731841.x.
9. **Kröger A, Biel S, Simon J, Gross R, Unden G, Lancaster CR.** 2002. Fumarate respiration of *Wolinella succinogenes*: enzymology, energetics and coupling mechanism. Biochim. Biophys. Acta **1553:**23–38. http://dx.doi.org/10.1016/S0005-2728(01)00234-1.
10. **Iverson TM, Luna-Chavez C, Croal LR, Cecchini G, Rees DC.** 2002. Crystallographic studies of the *Escherichia coli* quinol-fumarate reductase with inhibitors bound to the quinol-binding site. J. Biol. Chem. **277:**16124–16130. http://dx.doi.org/10.1074/jbc.M200815200.
11. **Yankovskaya V, Horsefield R, Törnroth S, Luna-Chavez C, Miyoshi H, Léger C, Byrne B, Cecchini G, Iwata S.** 2003. Architecture of succinate dehydrogenase and reactive oxygen species generation. Science **299:**700–704. http://dx.doi.org/10.1126/science.1079605.
12. **Iverson TM.** 2013. Catalytic mechanisms of complex II enzymes: a structural perspective. Biochim. Biophys. Acta **1827:**648–657. http://dx.doi.org/10.1016/j.bbabio.2012.09.008.
13. **Maklashina E, Iverson TM, Sher Y, Kotlyar V, Andréll J, Mirza O, Hudson JM, Armstrong FA, Rothery RA, Weiner JH, Cecchini G.** 2006. Fumarate reductase and succinate oxidase activity of Escherichia coli complex II homologs are perturbed differently by mutation of the flavin binding domain. J. Biol. Chem. **281:**11357–11365. http://dx.doi.org/10.1074/jbc.M512544200.
14. **Lancaster CR.** 2013. The di-heme family of respiratory complex II enzymes. Biochim. Biophys. Acta **1827:**679–687. http://dx.doi.org/10.1016/j.bbabio.2013.02.012.
15. **Berney M, Cook GM.** 2010. Unique flexibility in energy metabolism allows mycobacteria to combat starvation and hypoxia. PLoS One **5**(**1**): e8614. http://dx.doi.org/10.1371/journal.pone.0008614.
16. **Thauer RK, Jungermann K, Decker K.** 1977. Energy conservation in chemotrophic anaerobic bacteria. Bacteriol. Rev. **41:**100–180.
17. **Hågerhåll C.** 1997. Succinate:quinone oxidoreductases. Variations on a conserved theme. Biochim. Biophys. Acta **1320:**107–141. http://dx.doi.org/10.1016/S0005-2728(97)00019-4.
18. **Lancaster CR.** 2001. Succinate:quinone oxidoreductases—what can we learn from *Wolinella succinogenes* quinol:fumarate reductase? FEBS Lett. **504:**133–141. http://dx.doi.org/10.1016/S0014-5793(01)02706-5.
19. **Hågerhåll C, Aasa R, von Wachenfeldt C, Hederstedt L.** 1992. Two hemes in Bacillus subtilis succinate:menaquinone oxidoreductase (complex II). Biochemistry **31:**7411–7421. http://dx.doi.org/10.1021/bi00147a028.
20. **Lancaster CR, Kröger A.** 2000. Succinate:quinone oxidoreductases: new insights from X-ray crystal structures. Biochim. Biophys. Acta **1459:**422–431. http://dx.doi.org/10.1016/S0005-2728(00)00180-8.
21. **Schafer G, Anemuller S, Moll R.** 2002. Archaeal complex II: 'classical' and 'non-classical' succinate:quinone reductases with unusual features. Biochim. Biophys. Acta **1553:**57–73. http://dx.doi.org/10.1016/S0005-2728(01)00232-8.
22. **Hågerhåll C, Hederstedt L.** 1996. A structural model for the membrane-integral domain of succinate:quinone oxidoreductases. FEBS Lett. **389:**25–31. http://dx.doi.org/10.1016/0014-5793(96)00529-7.
23. **Bott M, Niebisch A.** 2003. The respiratory chain of *Corynebacterium glutamicum*. J. Biotechnol. **104:**129–153. http://dx.doi.org/10.1016/S0168-1656(03)00144-5.
24. **Nachlas MM, Margulies SI, Seligman AM.** 1960. A colorimetric method for the estimation of succinic dehydrogenase activity. J. Biol. Chem. **235:**499–503.
25. **Eoh H, Rhee KY.** 2013. Multifunctional essentiality of succinate metabolism in adaptation to hypoxia in *Mycobacterium tuberculosis*. Proc. Natl. Acad. Sci. U. S. A. **110:**6554–6559. http://dx.doi.org/10.1073/pnas.1219375110.
26. **Huang LS, Sun G, Cobessi D, Wang AC, Shen JT, Tung EY, Anderson VE, Berry EA.** 2006. 3-Nitropropionic acid is a suicide inhibitor of mitochondrial respiration that, upon oxidation by complex II, forms a covalent adduct with a catalytic base arginine in the active site of the enzyme. J. Biol. Chem. **281:**5965–5972. http://dx.doi.org/10.1074/jbc.M511270200.
27. **Griffin JE, Gawronski JD, Dejesus MA, Ioerger TR, Akerley BJ, Sassetti CM.** 2011. High-resolution phenotypic profiling defines genes essential for mycobacterial growth and cholesterol catabolism. PLoS Pathog. **7**(**9**): e1002251. http://dx.doi.org/10.1371/journal.ppat.1002251.
28. **Baek SH, Li AH, Sassetti CM.** 2011. Metabolic regulation of mycobacterial growth and antibiotic sensitivity. PLoS Biol. **9**(**5**):e1001065. http://dx.doi.org/10.1371/journal.pbio.1001065.
29. **Schirawski J, Unden G.** 1998. Menaquinone-dependent succinate dehydrogenase of bacteria catalyzes reversed electron transport driven by the proton potential. Eur. J. Biochem. **257:**210–215.
30. **Lemma E, Unden G, Kröger A.** 1990. Menaquinone is an obligatory component of the chain catalyzing succinate respiration in *Bacillus subtilis*. Arch. Microbiol. **155:**62–67. http://dx.doi.org/10.1007/BF00291276.
31. **Madej MG, Nasiri HR, Hilgendorff NS, Schwalbe H, Unden G, Lancaster CR, August RV, Re V, Recei M, October V, Goethe-universita JW, Gutenberg-universita J.** 2006. Experimental evidence for proton motive force-dependent catalysis by the diheme-containing succinate: menaquinone oxidoreductase from the Gram-positive bacterium *Bacillus licheniformis*. Biochemistry **45:**15049–15055. http://dx.doi.org/10.1021/bi0618161.
32. **Matsson M, Tolstoy D, Aasa R, Hederstedt L.** 2000. The distal heme center in *Bacillus subtilis* succinate:quinone reductase is crucial for electron transfer to menaquinone. Biochemistry **39:**8617–8624. http://dx.doi.org/10.1021/bi000271m.
33. **Hawkins BJ, Levin MD, Doonan PJ, Petrenko NB, Davis CW, Patel VV, Madesh M.** 2010. Mitochondrial complex II prevents hypoxic but not calcium- and proapoptotic Bcl-2 protein-induced mitochondrial membrane potential loss. J. Biol. Chem. **285:**26494–26505. http://dx.doi.org/10.1074/jbc.M110.143164.
34. **Rao SP, Alonso S, Rand L, Dick T, Pethe K.** 2008. The protonmotive force is required for maintaining ATP homeostasis and viability of hypoxic, nonreplicating *Mycobacterium tuberculosis*. Proc. Natl. Acad. Sci. U. S. A. **105:**11945–11950. http://dx.doi.org/10.1073/pnas.0711697105.
35. **Watanabe S, Zimmermann M, Goodwin MB, Sauer U, Barry CE, III, Boshoff HI.** 2011. Fumarate reductase activity maintains an energized membrane in anaerobic *Mycobacterium tuberculosis*. PLoS Pathog. **7**(**10**): e1002287. http://dx.doi.org/10.1371/journal.ppat.1002287.
36. **King A, Selak MA, Gottlieb E.** 2006. Succinate dehydrogenase and fumarate hydratase: linking mitochondrial dysfunction and cancer. Oncogene **25:**4675–4682. http://dx.doi.org/10.1038/sj.onc.1209594.
37. **Hoekstra AS, Bayley JP.** 2013. The role of complex II in disease. Biochim. Biophys. Acta **1827:**543–551. http://dx.doi.org/10.1016/j.bbabio.2012.11.005.
38. **Harada S, Inaoka DK, Ohmori J, Kita K.** 2013. Diversity of parasite complex II. Biochim. Biophys. Acta **1827:**658–667. http://dx.doi.org/10.1016/j.bbabio.2013.01.005.
39. **Kluckova K, Bezawork-Geleta A, Rohlena J, Dong L, Neuzil J.** 2013. Mitochondrial complex II, a novel target for anti-cancer agents. Biochim. Biophys. Acta **1827:**552–564. http://dx.doi.org/10.1016/j.bbabio.2012.10.015.
40. **Snapper SB, Melton RE, Mustafa S, Kieser T, Jacobs WR, Jr..** 1990. Isolation and characterization of efficient plasmid transformation mutants of *Mycobacterium smegmatis*. Mol. Microbiol. **4:**1911–1919. http://dx.doi.org/10.1111/j.1365-2958.1990.tb02040.x.
41. **Smeulders MJ, Keer J, Speight RA, Williams HD.** 1999. Adaptation of *Mycobacterium smegmatis* to stationary phase. J. Bacteriol. **181:**270–283.

42. **Parish T.** 2003. Starvation survival response of *Mycobacterium tuberculosis*. J. Bacteriol. **185:**6702–6706. http://dx.doi.org/10.1128/JB.185.22.6702-6706.2003.
43. **Berney M, Weimar MR, Heikal A, Cook GM.** 2012. Regulation of proline metabolism in mycobacteria and its role in carbon metabolism under hypoxia. Mol. Microbiol. **84:**664–681. http://dx.doi.org/10.1111/j.1365-2958.2012.08053.x.
44. **Larsen MH, Biermann K, Jacobs WR.** 2007. Laboratory maintenance of Mycobacterium tuberculosis. Curr. Protoc. Microbiol. Chapter 10:Unit 10A.1. http://dx.doi.org/10.1002/9780471729259.mc10a01s6.
45. **Sambrook J, Fritsch EF, Maniatis T.** 1989. Molecular cloning: a laboratory manual, 2nd ed. Cold Spring Harbor Laboratory Press, Cold Spring Harbor, NY.
46. **Sievers F, Wilm A, Dineen D, Gibson TJ, Karplus K, Li W, Lopez R, McWilliam H, Remmert M, Soding J, Thompson JD, Higgins DG.** 2011. Fast, scalable generation of high-quality protein multiple sequence alignments using Clustal Omega. Mol. Syst. Biol. **7:**539. http://dx.doi.org/10.1038/msb.2011.75.
47. **Gebhard S, Tran SL, Cook GM.** 2006. The Phn system of *Mycobacterium smegmatis*: a second high-affinity ABC-transporter for phosphate. Microbiology **152:**3453–3465. http://dx.doi.org/10.1099/mic.0.29201-0.
48. **Ho SN, Hunt HD, Horton RM, Pullen JK, Pease LR.** 1989. Site-directed mutagenesis by overlap extension using the polymerase chain reaction. Gene **77:**51–59. http://dx.doi.org/10.1016/0378-1119(89)90358-2.
49. **Pelicic V, Jackson M, Reyrat JM, Jacobs WR, Jr, Gicquel B, Guilhot C.** 1997. Efficient allelic exchange and transposon mutagenesis in *Mycobacterium tuberculosis*. Proc. Natl. Acad. Sci. U. S. A. **94:**10955–10960. http://dx.doi.org/10.1073/pnas.94.20.10955.
50. **Parish T, Stoker NG.** 2000. Use of a flexible cassette method to generate a double unmarked *Mycobacterium tuberculosis* tlyA plcABC mutant by gene replacement. Microbiology **146:**1969–1975.
51. **Lee MH, Pascopella L, Jacobs WR, Jr, Hatfull GF.** 1991. Site-specific integration of mycobacteriophage L5: integration-proficient vectors for *Mycobacterium smegmatis*, *Mycobacterium tuberculosis*, and bacille Calmette-Guerin. Proc. Natl. Acad. Sci. U. S. A. **88:**3111–3115.
52. **Parish T, Stoker NG.** 2000. *glnE* is an essential gene in *Mycobacterium tuberculosis*. J. Bacteriol. **182:**5715–5720. http://dx.doi.org/10.1128/JB.182.20.5715-5720.2000.
53. **Triccas JA, Parish T, Britton WJ, Gicquel B.** 1998. An inducible expression system permitting the efficient purification of a recombinant antigen from *Mycobacterium smegmatis*. FEMS Microbiol. Lett. **167:**151–156. http://dx.doi.org/10.1111/j.1574-6968.1998.tb13221.x.
54. **Robson J, McKenzie JL, Cursons R, Cook GM, Arcus VL.** 2009. The *vapBC* operon from *Mycobacterium smegmatis* is an autoregulated toxin-antitoxin module that controls growth via inhibition of translation. J. Mol. Biol. **390:**353–367. http://dx.doi.org/10.1016/j.jmb.2009.05.006.
55. **Timm J, Lim EM, Gicquel B.** 1994. *Escherichia coli*-mycobacteria shuttle vectors for operon and gene fusions to *lacZ*: the pJEM series. J. Bacteriol. **176:**6749–6753.
56. **Ackrell BA, Cochran B, Cecchini G.** 1989. Interactions of oxaloacetate with Escherichia coli fumarate reductase. Arch. Biochem. Biophys. **268:**26–34. http://dx.doi.org/10.1016/0003-9861(89)90561-4.
57. **Ackrell BA, Kearney EB, Singer TP.** 1978. Mammalian succinate dehydrogenase. Methods Enzymol. **53:**466–483. http://dx.doi.org/10.1016/S0076-6879(78)53050-4.
58. **Rao M, Streur TL, Aldwell FE, Cook GM.** 2001. Intracellular pH regulation by *Mycobacterium smegmatis* and *Mycobacterium bovis* BCG. Microbiology **147:**1017–1024.
59. **Schulz S, Iglesias-Cans M, Krah A, Yildiz O, Leone V, Matthies D, Cook GM, Faraldo-Gómez JD, Meier T.** 2013. A new type of Na(+)-driven ATP synthase membrane rotor with a two-carboxylate ion-coupling motif. PLoS Biol. **11**(6):e1001596. http://dx.doi.org/10.1371/journal.pbio.1001596.